Absolute transverse mobility and ratchet effect on periodic two-dimensional symmetric substrates

C. Reichhardt and C. J. Olson Reichhardt
Center for Nonlinear Studies and Theoretical Division, Los Alamos National Laboratory, Los Alamos, New Mexico 87545, USA
(Received 23 December 2002; revised manuscript received 29 July 2003; published 2 October 2003)

We present a simple model of an overdamped particle moving on a two-dimensional symmetric periodic substrate with a dc drive in the longitudinal direction and additional ac drives in both the longitudinal and transverse directions. For certain regimes we find that a finite longitudinal dc force produces a net dc response only in the transverse direction, which we term absolute transverse mobility. Additionally, we find regimes exhibiting a ratchet effect in the absence of an applied dc drive.

DOI: 10.1103/PhysRevE.68.046102 PACS number(s): 05.60.−k, 05.45.−a, 74.25.Qt, 87.16.Uv

I. INTRODUCTION

When an overdamped particle is driven with a dc drive, it moves in the direction of the drive, and in the absence of any other external force the particle velocity increases linearly with the drive. If there is some form of pinning from a substrate, then in general for a finite range of low drives the particle will be immobile or pinned [1,2]. For higher drives in the presence of pinning, the velocity versus force curves can be highly nonlinear [1,2]. For certain asymmetric substrate potentials, the particle speed can decrease with increasing applied drive, an effect that is termed negative differential resistance [3]. Such effects can also occur for collections of classical coupled particles interacting with periodic substrates [4]. In addition, a particle may exhibit a finite average dc velocity in the *absence* of any external dc drive. This is often referred to as a ratchet effect, which can be thermal [5] or deterministic [6]. Typically in ratchet systems there is some form of underlying asymmetric potential which leads to a spatial symmetry breaking if the potential is flashed or if an additional external ac drive is present. In the case of *absolute negative mobility*, when the particle is driven in the positive direction, its motion is in the *opposite* (negative) direction. Examples of this occur in ratchet systems composed of coupled particles, where the collective effects produce the negative mobility [7]. More recently a spatially symmetric two-dimensional (2D) system was found which exhibits absolute negative mobility for a *single* classical particle [8]. Many of these phenomena, such as negative differential resistance and absolute negative mobility, also occur in various semiconductor devices, where they arise due to quantum effects [9].

In a 2D system, there are additional possibilities for the motion of an overdamped particle which are not available in 1D systems. Under an external dc drive in the longitudinal or x direction, the response can be a finite velocity in the y or transverse direction only. We call such a phenomenon *absolute transverse mobility*.

In this work we present a simple model for a driven classical overdamped particle moving in a 2D *symmetric* potential that exhibits a variety of dynamical behaviors, including phase locking, absolute transverse mobility, and ratchet effects. Additionally, we find *reentrant* pinning phenomena where the moving particle becomes pinned upon increasing the drive. Our system consists of a particle moving over a symmetric periodic potential with an applied dc drive in the x direction and two additional ac drives in both the x and y directions. We set the amplitudes and frequencies for the two ac drives separately, and also consider highly nonlinear combinations of the ac drives which produce asymmetric closed orbits. In all cases, in the absence of a substrate and dc drive the average dc particle velocity is zero. Previous work on a similar system was performed with much simpler circular particle orbits, produced by setting the amplitudes of both ac drives equal to each other and fixing the phase difference at 90° [10].

In the previous work, several symmetrical phases were observed where the particle moves in both the transverse and longitudinal directions simultaneously when the dc drive is applied only in the longitudinal direction. In the current work we consider the case where the amplitudes or frequencies of the two ac drives are *different*. Here a far richer variety of classical closed orbits is realizable. The best examples of such orbits are Lissajous figures in which different sinusoidal orbits are plotted against one another.

Our results should apply to vortices moving in superconductors with periodic pinning arrays or Josephson junction arrays [11–15] when ac currents are applied in both the transverse and longitudinal directions. Additionally, the behavior described here should be observable in colloids moving over 2D periodic light arrays [16,17] or through dynamically manipulated arrays of holographic tweezers [18]. Further systems include biomolecules moving through periodic arrays of obstacles with two applied electric fields [19], electrons in a strong magnetic field moving through 2D antidot arrays with an additional ac drive to elongate one direction of the electron orbit [20], or ions moving in dissipative optical trap arrays [21] with ac applied fields. In the case of superconductors our results can also have applications for the controlled motion or removal of flux from superconductors and superconducting quantum interference devices. For colloids and biomolecules our results could provide a useful method for separating different particle species.

II. MODEL

In our model we consider an overdamped particle moving over a 2D periodic substrate. The equation of motion is

$$\mathbf{f}=\mathbf{f}_s+\mathbf{f}_{DC}+\mathbf{f}_{AC}=\eta\frac{d\mathbf{r}}{dt} \tag{1}$$

with the damping constant $\eta=1$. The assumption of overdamped motion should be valid for vortices in superconductors or Josephson junction arrays as well as for colloidal systems. The substrate consists of a periodic square array of obstacles with lattice constant a. The force from the substrate, composed of a fixed square array of repulsive particles, is $\mathbf{f}_s=\Sigma-\nabla U(x,y)$. This substrate can be realized in superconductors with a square periodic array of holes [11,12] or magnetic dots [14] when each site captures one vortex and additional vortices sit in the interstitial regions between the sites. The interstitial vortices move in a periodic potential created by the repulsive interaction from the pinned vortices so that $U(r)=F_0\ln(r)$ for $r\ll 2\lambda^2/d$. Here forces are measured in units of $F_0=\Phi_0^2 d/16\pi\lambda^2$, where Φ_0 is the flux quantum, d is the film thickness, and λ is the London penetration depth. This potential can be treated as in Ref. [22]. The motion of interstitial vortices has been directly imaged in experiments with this geometry [12], and phase-locking effects and dc and ac driven interstitial vortex motion have also been observed [13]. For most of the results presented here we use a system of size $8a\times 8a$. For larger systems we observe the same results, indicating that our system is large enough to capture the essential physics. We have tested different initial conditions by placing the particle at different locations at the start of the simulations and find that the general results are unchanged. Additionally, we have considered other potentials, such as those created by fixed Coulomb charges or Yukawa potentials, and find that they produce the same phases.

Throughout this work the dc drive $\mathbf{f}_{DC}=f_{DC}\hat{\mathbf{x}}$ is applied along the positive longitudinal (x direction) symmetry axis of the pinning array. The ac drive is applied in both the x and y directions and is given by

$$\mathbf{f}_{AC}=A\sin(\omega_A t)\hat{\mathbf{x}}-B\cos(\omega_B t)\hat{\mathbf{y}}. \tag{2}$$

Note that there is *no* dc driving component in the transverse or y direction. In the first part of this work we set $\omega_A=\omega_B$, fix $B=0.24$, and vary A. For $A=B$ the particle moves in a clockwise circle just large enough to encircle one maximum of the substrate potential. As A decreases the particle orbit becomes elliptical with the long side in the y direction. We monitor the time averaged particle velocity $V_x=(1/TN)\Sigma_{t=0}^{T}\Sigma_{i=0}^{N}v_i(t)\cdot\hat{\mathbf{x}}$, where T is the period and N is the number of particles, and similarly the time averaged transverse velocity V_y as $\mathbf{f}_{DC}$ is increased from 0 to 1.0 in increments of 2.5×10^{-4}, with 3×10^5 time steps spent at each drive to ensure a steady state. Time is measured in units of $t_0=\eta/F_0$. We also investigate $\omega_B\neq\omega_A$ for varied ac amplitude. In this case we find a ratchet effect.

III. ABSOLUTE TRANSVERSE MOBILITY

In Fig. 1 we plot V_x (heavy line) and V_y (light line) versus f_{DC} for different values of A/B at fixed $\omega_A/\omega_B=1$ and $a=1.42\lambda$. In Fig. 1(a), at $A/B=0.875$, $V_x=0$ for $f_{DC}<0.03$, indicating that the particle is pinned in the x direction. For $f_{DC}\geqslant 0.03$, V_x increases in a series of steps of height $a\omega$. These steps are a signature of the phase locking which occurs due to resonances between the applied ac frequency and the washboard frequency generated as the particle moves over the periodic substrate. As shown in Fig. 1(a), V_y has a finite value of $V_y=a\omega$ for $f_{DC}<0.03$, indicating that even though the dc drive is strictly in the x direction the particle is moving *strictly* in the y direction. In analogy with the phenomena of absolute negative mobility, where a particle moves in the opposite direction of an applied driving force, we term the strictly y-direction motion absolute transverse mobility. For large enough drives, $f_{DC}\geqslant 0.16$, the motion is strictly in the x direction. At intermediate drives, $0.03<f_{DC}<0.16$, different dynamical phases appear. For $0.045<f_{DC}<0.065$ the particle moves in the x direction only, while for $0.07<f_{DC}<0.158$, $V_x=V_y$, indicating that the particle is moving at 45° with respect to the drive. There is also a small region near $f_{DC}=0.035$ where 45° motion occurs. In Fig. 1(b), for $A/B=0.625$ there is a clear *pinned* phase at low f_{DC} where both V_x and V_y are zero. As we increase the drive, we observe the same phases shown in Fig. 1(a), with the boundaries shifted. Near the transitions of these phases, smaller steps in V_x and V_y can occur with height $pa\omega/q$ where p and q are integers. In Fig. 1(c), for $A/B=0.375$, 45° motion no longer appears. Instead, there is a remarkable *reentrant* pinned phase for $0.1385<f_{DC}<0.148$. As f_{DC} increases, the particle is first pinned, then moves in the y direction, is repinned, and finally moves in the x direction.

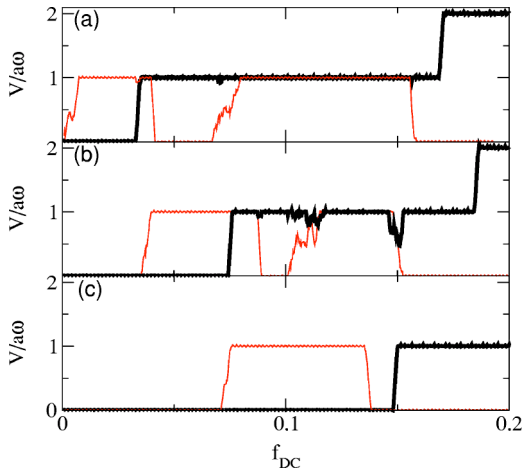

FIG. 1. The longitudinal particle velocity $V_x/a\omega$ (heavy lines) and transverse particle velocity $V_y/a\omega$ (light lines) vs applied dc drive $\mathbf{f}_{DC}=f_{DC}\hat{\mathbf{x}}$ for ac amplitudes (a) $A/B=0.875$, (b) $A/B=0.625$, and (c) $A/B=0.375$.

We next consider the particle trajectories in these different phases. We term the pinned regime phase I_p, the absolute transverse mobility regime phase II_y, the 45° motion regime phase $\mathrm{III}_{x\text{-}y}$, and the strictly x-direction motion phase IV_x. In Fig. 2 we illustrate these phases for fixed values of f_{DC} from the system in Fig. 1(a) with $A/B=0.875$. The black lines are the trajectories of the moving particle and the black

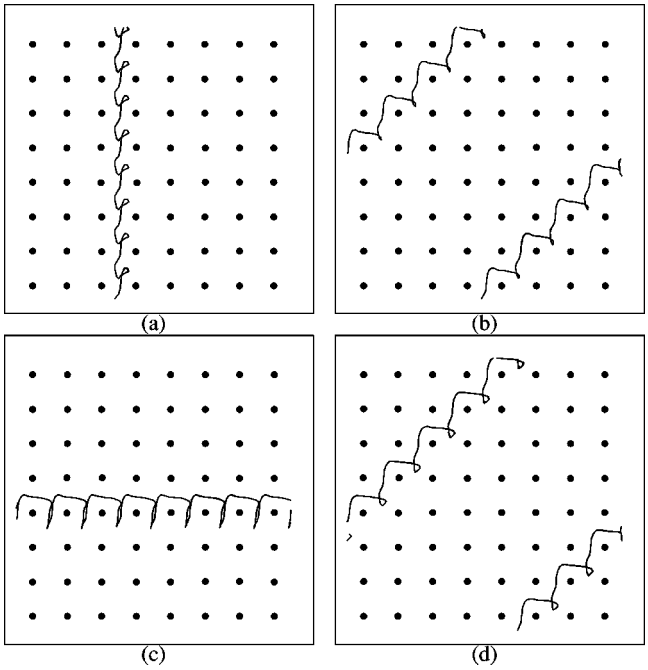

FIG. 2. The particle trajectories (black lines) for a fixed time interval for the system in Fig. 1(a) with $A/B=0.875$. The black dots are the potential maxima of the periodic substrate. (a) $f_{DC}=0.025$, phase II_y; (b) $f_{DC}=0.0375$, phase $\mathrm{III}_{x\text{-}y}$; (c) $f_{DC}=0.06$, phase IV_x; and (d) $f_{DC}=0.125$, phase $\mathrm{III}_{x\text{-}y}$.

dots are the potential maxima of the underlying periodic substrate. Figure 2(a) shows the trajectory of the moving particle in phase II_y at $f_{DC}=0.025$. In every period the particle makes a small loop, but the net motion of the particle is in the positive y direction only. In phase $\mathrm{III}_{x\text{-}y}$, shown in Fig. 2(b) for $f_{DC}=0.0375$, the particle moves equal distances in the x and y directions. At $f_{DC}=0.06$, illustrated in Fig. 2(c), the phase IV_x motion is strictly in the x direction, and the particle translates a distance a every period. In Fig. 2(d) we show the reentrant phase $\mathrm{III}_{x\text{-}y}$ flow for $f_{DC}=0.125$, very similar to that seen in Fig. 2(b). For higher drives $f_{DC}>0.16$, the motion is strictly in the x direction and is similar to Fig. 2(c).

For the simulations shown in Figs. 1 and 2, the particle initially begins in the center of the plaquette with zero-dc drive. We considered the effect of both using different starting locations and setting f_{DC} to a finite initial value. In each case we find that the particle quickly settles into a regular orbit. The orbits that appear when V_x or V_y is constant correspond to the same periodic, phase-locked attractor orbits that were obtained previously in Figs. 1 and 2. We do find some nonperiodic orbits in the regions where V_x or V_y are not constant, such as in the transition regimes between the different phases.

We performed a series of simulations at different values of A/B to identify the onset of the four phases as a function of f_{DC}. In Fig. 3 we present the resulting dynamic phase diagram A/B versus f_{DC} which shows a very rich structure. For $A/B=0$ the system depins directly into phase IV_x and there are no phases that involve motion in the y direction. Phase II_y first occurs for $A/B>0.03$, and gradually increases

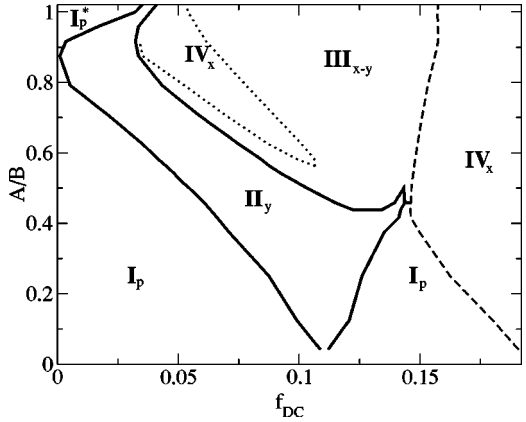

FIG. 3. Dynamic phase diagram for A/B vs f_{DC} for a system with $\omega_A=\omega_B$. Phase I_p: pinned phase. Phase II_y: motion only in the y direction. Phase $\mathrm{III}_{x\text{-}y}$: motion at 45°. Phase IV_x: motion only in the x direction.

in width until $A/B\approx 0.43$, when phase $\mathrm{III}_{x\text{-}y}$ appears. The reentrant pinning phase I_p decreases in size and then disappears over this same interval. There is also a small region around $A/B\gtrsim 0.43$ where phase II_y and phase $\mathrm{III}_{x\text{-}y}$ are both reentrant. A reentrant tongue of phase IV_x at low drives appears for $A/B>0.55$. At all values of A/B, the flow at large f_{DC} is strictly in the x direction (phase IV_x). The width of the pinned phase I_p^* increases upon approaching $A/B=1$ from below since the almost circular particle orbit around one potential maximum is highly stable. Motion in the y direction (phase II_y) still appears for the symmetric ac drive $A/B=1$ due to the fact that the particular chirality of the ac drive breaks the reflection symmetry across the y axis.

For $A/B>0.6$, the sliver of reentrant phase $\mathrm{III}_{x\text{-}y}$ falling between phases II_y and IV_x becomes gradually smaller as A/B increases until it vanishes above $A/B=0.88$. The transition from phase II_y to phase IV_x at higher values of $A/B>0.88$ occurs in a very small window of f_{DC} but is not completely sharp. Instead there is a small region where the flowing particle moves in both the x and y direction but at an angle less than 45°. The flow is intermittent and jumps among different orbits or angles. We have also considered the effect of starting the particle at a nonzero fixed f_{DC} in the transition region between phases II_y and IV_x and find that the flow will settle quickly to phase II_y or IV_x.

We now consider the conditions under which transverse mobility and the reentrant pinning can occur, and indicate where the boundaries between the different phases are expected to fall.

Pinned phases I_p and I_p^*. The particle remains in the pinned phase I_p as long as the combined dc and maximum ac components are less than the confining barrier produced by the repulsive obstacles. This barrier has a strong angular dependence due to its egg-carton shape, and the lowest points of the barrier fall at the center of each of the four sides of the plaquette, at $x_{\min}^{\pm}$ and $y_{\min}^{\pm}$, where the x- or y-confining forces pass through a minimum. The largest thresholds occur for a particle trajectory along a 45° angle passing through the potential maximum. At $A/B\approx 0.88$, a transition to a new pinned

phase I_p^* occurs. For $A/B<0.88$, the pinned particle orbit is contained inside a single plaquette. For $A/B>0.88$, the orbit becomes too large to fit inside the plaquette, and the particle switches to a larger orbit centered around one of the potential maxima.

Transition from I_p to II_y. For $A=0$ and fixed B, the particle orbit consists of a single line extending from the top to the bottom of the plaquette, close to the minimum y-confining force points of the potential, $y_{\min}^{\pm}$. Due to this proximity induced by the y component of the ac drive, the particle depins in the y direction *before* it depins in the x direction for nonzero values of A, and enters phase II_y. The particle hops from one plaquette to the next plaquette in the positive y direction during a brief interval at the end of the rising phase of the particle orbit. In order to make this hop, the particle must be moving rapidly enough to reach the next plaquette before the ac phase reaches the downward portion of the cycle. Increasing f_{DC} or increasing A both contribute to increasing the velocity of the particle during the hop. The minimum f_{DC} value required to permit the particle to hop at low but nonzero A is $f_{DC}\approx 0.11$. As A/B increases, the x component of the ac force also contributes to the particle velocity during the hop, so the value of f_{DC} that must be applied to induce y direction motion drops, such that the particle velocity during the hop at the onset of phase II_y remains roughly constant as A/B increases.

Transition from II_y to I_p. As f_d increases further within phase II_y, for $A/B<0.45$, a transition to a reentrant pinned phase occurs. Here, the x velocity of the particle has increased enough so that the particle is swept past the minimum in the y-confining potential $y_{\min}^{+}$ before it has time to hop to the next plaquette. Thus the particle returns to a pinned orbit. The II_y-I_p transition line moves to higher f_d with increasing A/B due to the fact that the time required for the particle to complete its hop to the next plaquette drops as A/B increases. Therefore, a higher f_{DC} is required to sweep the particle past $y_{\min}^{+}$ before the hop is complete.

Transition from I_p to IV_x. Beyond the second pinned phase I_p, as f_{DC} is further increased, the particle orbit is shifted closer to the minimum in the x-confining potential on the right side of the plaquette, $x_{\min}^{+}$, and when the combined ac and dc forces in the x direction exceed the potential strength at this minimum, the particle depins in the positive x direction. For $A/B<0.45$, f_{DC} at the depinning transition decreases with increasing A/B due to the fact that the ac force also contributes to the net x-force on the particle. This contribution saturates at $A/B\approx 0.45$, when the II_y-I_p line meets the I_p-IV_x line and the reentrant phase disappears.

Transition from II_y to IV_x, with a reentrant $III_{x\text{-}y}$. For $A/B>0.45$, as f_{DC} is increased, the particle motion leaves phase II_y, passing briefly through a sliver of phase $III_{x\text{-}y}$ before entering phase IV_x, with motion in the x direction only. Depinning of the particle in the x direction first occurs when the x component of the ac drive combined with f_{DC} exceeds the x confining force of the potential at $x_{\min}^{+}$. At this value of f_{DC}, the particle is moving in both the x and y directions in phase $III_{x\text{-}y}$. Due to the x-motion of the particle, however, the y motion becomes unstable, and at slightly higher values of f_{DC}, the y motion ends and the particle moves only in the x direction in phase IV_x. As the drive is further increased, stable y motion becomes possible again, and the particle enters a wide region of phase $III_{x\text{-}y}$.

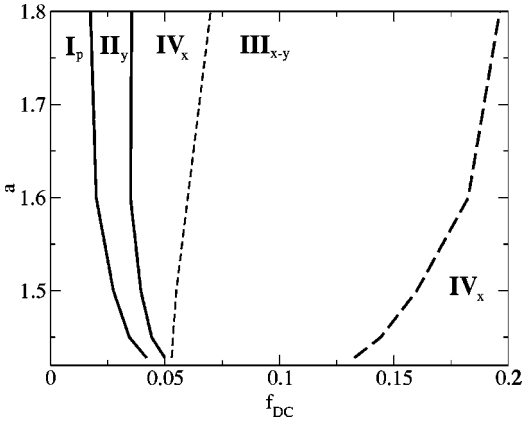

FIG. 4. Dynamic phase diagram for substrate lattice constant a vs f_{DC} for a system with $A=B$ and $\omega_A=\omega_B$. Phase I_p: pinned phase. Phase II_y: motion only in the y direction. Phase $III_{x\text{-}y}$: motion at 45°. Phase IV_x: motion only in the x direction.

Transition from $III_{x\text{-}y}$ to IV_x at high f_{DC}. As f_{DC} is increased further, the y direction motion of phase $III_{x\text{-}y}$ ends when the particle orbit becomes so extended in the x direction due to the increased f_{DC} that it can no longer depin in the y direction since it has moved away from the y minimum location $y_{\min}^{+}$.

We next consider the effect of changing the density of the system. We achieve this by performing a series of simulations for fixed $A/B=1.0$ while varying the lattice constant of the periodic substrate and changing the system size accordingly. This increases the effective substrate strength since it increases the barrier to hop from one plaquette to another. In Fig. 4 we show the phase diagram of the substrate lattice constant a versus f_{DC}. We consider lattice constants ranging from 1.42λ to 1.8λ. New dynamic phases appear for lattice constants outside this range. For smaller lattice constants $a<1.42$, the zero-dc drive orbits start to encircle two or more potential maxima. For larger lattice constants, $a>1.8$, the phases start to show disordered or chaotic behavior, and phases I_p to IV_x become difficult to define. Figure 4 shows that the width of the pinned phase I_p grows for denser systems, as expected due to the increased barriers for interplaquette jumps. It might be expected that phase II_y would grow for smaller a as the plaquettes shrink; however, the increased repulsion caused by the shorter distance between the potential maxima and the particle causes the particle orbit to shrink as well. Phase II_y and the first phase IV_x both shrink with decreasing a, while the second onset of phase IV_x occurs at a lower value of f_{DC} since the particle does not need to move as far in the x direction in order to reach the next plaquette.

We have also considered the effects of adding a phase shift to the ac drives. We shift the phase of the x component of the ac drive by δ: $A\sin(\omega_A t+\delta)\hat{\mathbf{x}}$. This causes the particle orbits to become tilted and elliptical. We restrict ourselves to

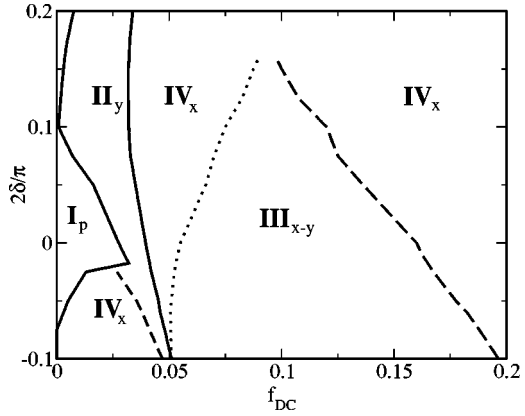

FIG. 5. Dynamic phase diagram for the phase shift δ in units of $2/\pi$ vs f_{DC} for a system with $\omega_A=\omega_B$ and $A=B$. The phase shift is added to the x component of the ac drive. Phase I_p: pinned phase. Phase II_y: motion only in the y direction. Phase $III_{x\text{-}y}$: motion at 45°. Phase IV_x: motion only the in the x direction.

the region $-0.05/\pi<\delta<0.1/\pi$ in phase space where the four phases described above occur. For larger shifts new phases can arise. In Fig. 5 we plot the phase diagram as a function of phase shift δ versus f_{DC}. At $\delta=\pi/2$ the ac orbit would be a straight line along 45°. Figure 5 shows that as δ increases from zero, which corresponds to the elliptical orbit being tilted toward the right, phase II_y increases in size and phase I_p decreases in size. For large enough shifts δ, phase $III_{x\text{-}y}$ disappears. For negative phase shifts a new region of phase IV_x appears between phases I_p and II_y. For large enough negative phase shifts we observe a ratchet effect in which the particle moves in the x direction with zero-dc drive. We discuss this more in the following section. Also for increasing negative phase shifts, phase II_y decreases in size while phase $III_{x\text{-}y}$ increases in size.

IV. RATCHET EFFECTS

The elliptical ac drives in the preceding sections preserve the combined x and y reflection symmetries of the system. The ac drives with additional asymmetries can produce a net dc motion or ratchet effect in the absence of a dc drive. We consider a system with $f_{DC}=0$ under an asymmetric applied ac drive of the form

$$\mathbf{f}_{AC}=A[\sin(\omega_A t)+\sin^3(\omega_B t)]\hat{\mathbf{x}}-B\cos(\omega_B t)\hat{\mathbf{y}}, \qquad (3)$$

where $\omega_B/\omega_A=0.8$. In Fig. 6(a) we plot V_y versus A for constant $B=0.34$ and $f_{DC}=0$. In this regime, $V_x=0$. There are a series of regions for increasing A that have a finite dc value of V_y in both the positive and negative directions, indicating a ratchet effect with velocity $a\omega_B/2$. In Fig. 6(c) we illustrate a positive V_y orbit from the system in Fig. 6(a) at $A=0.285$. The orbit has alternating lobes which are angled in the positive y direction. In Fig. 6(d) we show that the negative V_y orbit at $A=0.5$ is composed of an alternating double rectangular orbit which is tilted in the negative y direction.

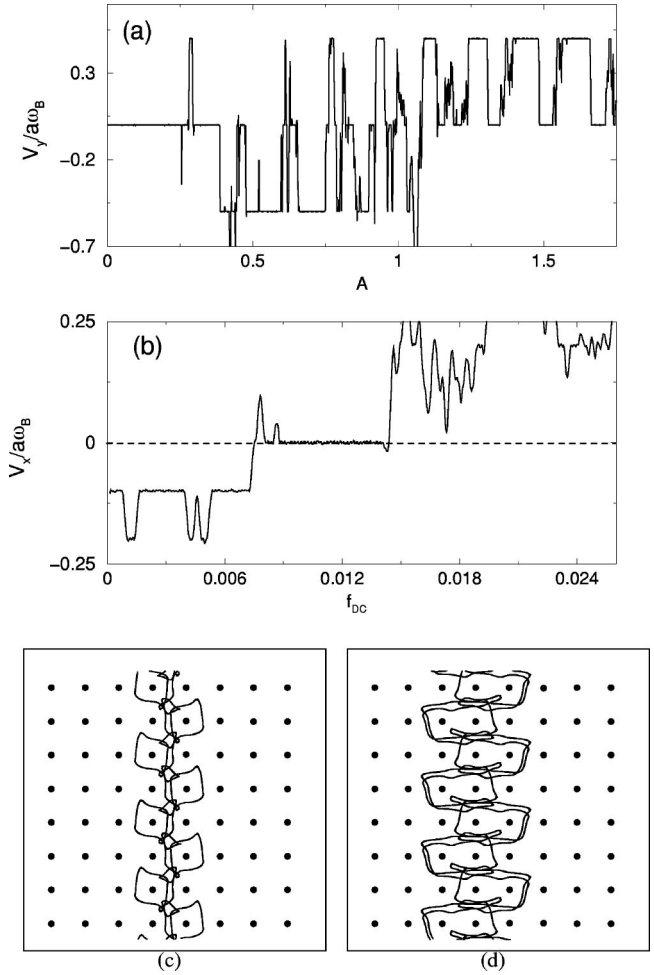

FIG. 6. (a) Transverse velocity $V_y/a\omega_B$ vs A at $f_{DC}=0$ and $B=0.34$ for a system with an asymmetric ac drive, $\omega_B/\omega_A=0.8$. (b) Longitudinal velocity V_x vs f_{DC} for a system at $B/A=0.7$ showing a negative ratchet effect at $f_{DC}<0.0075$. (c) Particle trajectory for a positive V_y orbit from panel (a) at $A=0.285$, $B=0.34$, and $f_{DC}=0$. (d) Particle trajectory for a negative V_y orbit from panel (a) at $A=0.5$, $B=0.34$, and $f_{DC}=0$.

We have also found ratchet regimes where there is a finite dc velocity in the *opposite* direction of the applied dc drive. In Fig. 6(b), we plot V_x versus f_{DC} for a system with $\mathbf{f}_{AC}=A\sin(\omega_A t)\hat{\mathbf{x}}-B\cos(\omega_B t)\hat{\mathbf{y}}$, $B/A=0.7$, and $\omega_A/\omega_B=1.85$. Here there is a regime $0<f_{DC}<0.0075$ where the particle is moving *backward* with respect to the dc drive, which is applied in the positive x direction. The system enters a pinned phase for $0.009<f_{DC}<0.014$ before beginning to move strictly in the positive x direction for $f_{DC}>0.014$. We note that this negative velocity in opposition to the dc drive is not a negative mobility regime. Instead, it is a ratchet effect which can persist for a range of opposite dc drive. The fact that there is a finite negative velocity even at $f_{DC}=0.0$, as seen in Fig. 6(b), shows that the dc drive is not causing the net dc motion.

A basic question is what are the minimal ac drive criteria required to produce a ratchet effect at $f_{DC}=0.0$. In general we find that ratchet effects occur for ac drives in which at least one of the spatial reflection symmetries is broken.

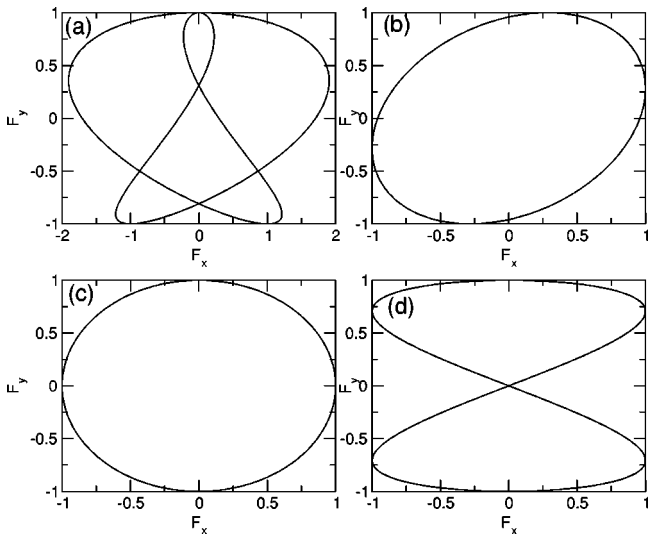

FIG. 7. (a) and (b) F_x vs F_y for ac drives that produce a ratchet effect. (a) $\mathbf{f}_{AC}=A\sin(\omega_A t)\hat{\mathbf{x}}+A\sin(1.5\omega_A t)\hat{\mathbf{x}}-B\cos(1.5\omega_B t)\hat{\mathbf{y}}$, $A/B=1$, $A=1$, and $\omega_A/\omega_B=1$. (b) A ratchet effect produced by a phase shift: $\mathbf{f}_{AC}=A\sin(\omega_A t+\delta)\hat{\mathbf{x}}-B\cos(\omega_B t)$, $\delta=0.287$, $A/B=1$, and $\omega_A/\omega_B=1$. (c) and (d) F_x vs F_y for ac drives that do not produce a ratchet effect. (c) $\mathbf{f}_{AC}=A\sin(\omega_A t)\hat{\mathbf{x}}-B\cos(\omega_B t)\hat{\mathbf{y}}$ with $A/B=1$ and $\omega_A/\omega_B=1$. (d) $\mathbf{f}_{AC}=A\sin(\omega_A t)\hat{\mathbf{x}}-B\cos(2\omega_B t)\hat{\mathbf{y}}$ with $A/B=1$ and $\omega_A/\omega_B=1$.

An example of a simple ac drive that produces a zero-dc ratchet effect is $\mathbf{f}_{AC}=A\sin(\omega_A t)\hat{\mathbf{x}}+A\sin(1.5\omega_A t)\hat{\mathbf{x}}-B\cos(1.5\omega_B t)\hat{\mathbf{y}}$, with $A/B=1$ and $\omega_A/\omega_B=1$. In Fig. 7(a) we plot F_x versus F_y for this ac drive in the absence of a substrate with $A=1.0$. In Fig. 8(a) we show the particle motion over the substrate for $f_{DC}=0.0$. The particle translates in the negative y direction. Figure 7(a) shows that the ac drive breaks a spatial symmetry across the y axis. The orbit of the particle thus breaks an x-axis symmetry. In Fig. 7(c) we plot F_x versus F_y for $\mathbf{f}_{AC}=A\sin(\omega_A t)\hat{\mathbf{x}}-B\cos(\omega_B t)\hat{\mathbf{y}}$ with $A/B=1$ and $\omega_A/\omega_B=1$, and in Fig. 7(d) we plot F_x versus F_y for $\mathbf{f}_{AC}=A\sin(\omega_A t)\hat{\mathbf{x}}-B\cos(2\omega_B t)\hat{\mathbf{y}}$ with $A/B=1$ and $\omega_A/\omega_B=1$. These drives do not produce a zero-dc ratchet effect, and these orbits do not break a reflection symmetry. As indicated in the phase diagram of Fig. 6, the addition of a phase shift to the ac drive in the x direction produces another simple ac drive that exhibits a zero-dc ratchet effect. In Fig. 8(b) we show a particle orbit under the addition of a negative phase shift, $\mathbf{f}_{AC}=A\sin(\omega_A t+\delta)\hat{\mathbf{x}}-B\cos(\omega_B t)$ with $\delta=0.287$, $A/B=1$, and $\omega_A/\omega_B=1$, that produces a zero-dc ratchet effect in the x direction. F_x versus F_y for this orbit is illustrated in Fig. 7(b). The ac drive in Fig. 7(b) breaks both the x and y reflection symmetries. We note that even if an ac drive breaks a reflection symmetry it does not necessarily produce a zero-dc ratchet. However, we have never observed zero-dc ratcheting for symmetrical ac drives.

V. SUMMARY

We have presented a simple model of a particle driven in a two-dimensional symmetric periodic substrate with an elliptical ac drive. In certain regimes, the particle moves strictly in the y direction when the dc drive is applied in the x direction. We term this effect absolute transverse mobility.

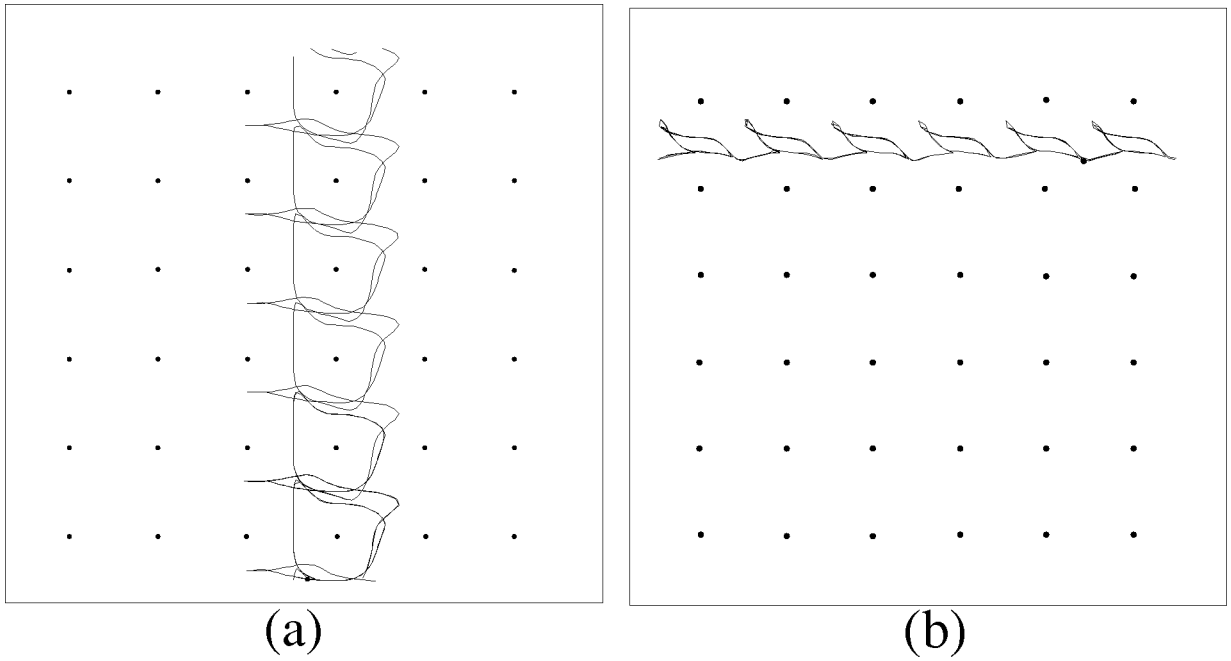

FIG. 8. The particle trajectories (black line) for a fixed time interval and $f_{DC}=0.0$ for motion in a 2D periodic substrate with potential maxima located at the black dots. (a) A ratchet effect due to the breaking of a reflection symmetry. The particle moves in the negative y direction when driven with the ac drive shown in Fig. 7(a): $\mathbf{f}_{AC}=A\sin(\omega_A t)\hat{\mathbf{x}}+A\sin(1.5\omega_A t)\hat{\mathbf{x}}-B\cos(1.5\omega_B t)\hat{\mathbf{y}}$, $A/B=1$, and $\omega_A/\omega_B=1$. (b) A ratchet effect produced by the addition of a phase shift. The particle moves in the positive x direction when driven with the ac drive shown in Fig. 7(b): $\mathbf{f}_{AC}=A\sin(\omega_A t+\delta)\hat{\mathbf{x}}-B\cos(\omega_B t)$, $\delta=0.287$, $A/B=1$, and $\omega_A/\omega_B=1$.

Additionally, we have mapped several dynamic phase diagrams for this system, which feature a number of dynamical phases including simultaneous motion in the x and y directions, as well as a reentrant pinned phase. For ac drives which produce asymmetric orbits, net dc motion or a zero-dc ratchet effect can arise in the absence of an applied dc drive. Our results can be tested experimentally and have useful applications for controlling flux motion in superconductors, colloids in optical trap arrays, and biomolecules moving through a periodic obstacle array.

ACKNOWLEDGMENTS

We thank C. Bechinger, D. Grier, M. B. Hastings, and P. Korda for useful discussions. This work was supported by the U.S. DOE under Contract No. W-7405-ENG-36.

[1] G. Grüner, Rev. Mod. Phys. **60**, 1129 (1988).
[2] G. Blatter, M.V. Feigel'man, V.B. Geshkenbein, A.I. Larkin, and V.M. Vinokur, Rev. Mod. Phys. **66**, 1125 (1994).
[3] G.A. Cecchi and M.O. Magnasco, Phys. Rev. Lett. **76**, 1968 (1996).
[4] C. Reichhardt, C.J. Olson, and F. Nori, Phys. Rev. B **58**, 6534 (1998).
[5] M.O. Magnasco, Phys. Rev. Lett. **71**, 1477 (1993); R.D. Astumian and M. Bier, *ibid.* **72**, 1766 (1994); C.R. Doering, W. Horsthemke, and J. Riordan, *ibid.* **72**, 2984 (1994); P. Reimann, Phys. Rep. **361**, 57 (2002).
[6] R. Bartussek, P. Hänggi, and J.C. Kissner, Europhys. Lett. **28**, 459 (1994); J.L. Mateos, Phys. Rev. Lett. **84**, 258 (2000).
[7] P. Reimann, R. Kawai, C. van den Broeck, and P. Hänggi, Europhys. Lett. **45**, 545 (1999); J. Buceta, J.M. Parrondo, C. Van den Broeck, and F.J. de la Rubia, Phys. Rev. E **61**, 6287 (2000); B. Cleuren and C. Van den Broeck, Europhys. Lett. **54**, 1 (2001).
[8] R. Eichhorn, P. Reimann, and P. Hänggi, Phys. Rev. Lett. **88**, 190601 (2002); Phys. Rev. E **66**, 066132 (2002).
[9] K. Seeger, *Semiconductor Physics* (Springer-Verlag, Berlin, 1982); E. Scholl, *Nonequilibrium Phase Transitions in Semiconductors* (Springer-Verlag, Berlin, 1987); S. Wang and D.D.L. Chung, Composites, Part B **30**, 579 (1999).
[10] C. Reichhardt, C.J. Olson, and M.B. Hastings, Phys. Rev. Lett. **89**, 024101 (2002).
[11] M. Baert, V.V. Metlushko, R. Jonckheere, V.V. Moshchalkov, and Y. Bruynseraede, Phys. Rev. Lett. **74**, 3269 (1995); S.B. Field, S.S. James, J. Barentine, V. Metlushko, G. Crabtree, H. Shtrikman, B. Ilic, and S.R.J. Brueck, *ibid.* **88**, 067003 (2002).
[12] K. Harada, O. Kamimura, H. Kasai, T. Matsuda, A. Tonomura, and V.V. Moshchalkov, Science **274**, 1167 (1996).
[13] L. Van Look, E. Rosseel, M.J. Van Bael, K. Temst, V.V. Moshchalkov, and Y. Bruynseraede, Phys. Rev. B **60**, R698 (1999).
[14] J.I. Martín, M. Vélez, A. Hoffmann, I.K. Schuller, and J.L. Vicent, Phys. Rev. Lett. **83**, 1022 (1999).
[15] C. Reichhardt, A.B. Kolton, D. Domínguez, and N. Grønbech-Jensen, Phys. Rev. B **64**, 134508 (2001).
[16] P.T. Korda, M.B. Taylor, and D.G. Grier, Phys. Rev. Lett. **89**, 128301 (2002).
[17] M. Brunner and C. Bechinger, Phys. Rev. Lett. **88**, 248302 (2002); K. Mangold, P. Leiderer, and C. Bechinger, *ibid.* **90**, 158302 (2003).
[18] J.E. Curtis, B.A. Koss, and D.G. Grier, Opt. Commun. **207**, 169 (2002).
[19] W.D. Volkmuth and R.H. Austin, Nature (London) **358**, 600 (1992); C.-F. Chou, O. Bakajin, S.W.P. Turner, T.A.J. Duke, S.S. Chan, E.C. Cox, H.G. Craighead, and R.H. Austin, Proc. Natl. Acad. Sci. U.S.A. **96**, 13 762 (1999); J.-L. Vioy, Rev. Mod. Phys. **72**, 813 (2000).
[20] D. Weiss, M.L. Roukes, A. Menschig, P. Grambow, K. von Klitzing, and G. Weimann, Phys. Rev. Lett. **66**, 2790 (1991); G.R. Nash, S.J. Bending, M. Riek, and K. Eberl, Phys. Rev. B **63**, 113316 (2001); W. Breuer, D. Weiss, and V. Umansky, Physica E (Amsterdam) **12**, 216 (2002).
[21] G. Grynberg and C. Robilliard, Phys. Rep. **5-6**, 335 (2001); M. Schiavoni, F.-R. Carminati, L. Sanchez-Palencia, F. Renzoni, and G. Grynberg, Europhys. Lett. **59**, 493 (2002).
[22] N. Grønbech-Jensen, Int. J. Mod. Phys. C **7**, 873 (1996).